Biocompatible stimuli – responsive W/O/W multiple emulsions prepared by one – step mixing with a single diblock copolymer emulsifier

AUTHOR NAMES

Marine Protat[1, 2], Noémie Bodin[1, 2], Frédéric Gobeaux[2], Florent Malloggi[2], Jean Daillant[3], Nadège Pantoustier[1, 4], Patrick Guenoun[2], Patrick Perrin[1, 4]**

AUTHOR ADDRESS

1. Sciences et Ingénierie de la Matière Molle, UMR CNRS 7615, ESPCI ParisTech, PSL Research University, 10 rue Vauquelin, Paris, 75005, France.

2. LIONS, NIMBE, CEA, CNRS, Université Paris-Saclay, CEA Saclay 91191 Gif-sur-Yvette Cedex, France.

3. Synchrotron Soleil, L'Orme des Merisiers, Saint-Aubin – BP 48, 91192 Gif-sur-Yvette Cedex, France.

4. Sorbonne-Universités, UPMC Université Paris 06, SIMM, 10 rue Vauquelin, Paris 75005, France.

KEYWORDS

Multiple emulsions, amphiphilic block copolymer, stimuli-responsive, phase inversion, interfaces

ABSTRACT

Multiple water-in-oil-in-water (W/O/W) emulsions are promising materials to design carriers of hydrophilic molecules or drug delivery systems, provided stability issues are solved and biocompatible chemicals can be used. In this work, we designed a biocompatible amphiphilic copolymer poly(dimethylsiloxane)-*b*-poly(2-(dimethylamino)ethyl methacrylate) (PDMS-*b*-PDMAEMA) that can stabilize emulsions made with various biocompatible oils. The hydrophilic/hydrophobic properties of the copolymer can be adjusted using both pH and ionic strength stimuli. Consequently, the making of O/W (oil in water), W/O (water in oil), and W/O/W emulsions can be achieved by sweeping pH and ionic strength. Of importance, W/O/W emulsions are formulated over a large pH and ionic strength domain in a one-step emulsification process via transitional phase inversion and are stable for several months. A Cryo-TEM and interfacial tension studies show that the formation of these W/O/W emulsions is likely to be correlated to the interfacial film curvature and microemulsion morphology.

INTRODUCTION

Multiple emulsions like water-in-oil-in-water emulsions (W/O/W) are an ideal platform for the encapsulation of many molecules of interest that need to be protected from external stresses before being released. In the food processing industry, the high potential of multiple emulsions to encapsulate and protect sensitive and reactive compounds such as flavors, vitamins or minerals has been demonstrated[1–3]. Multiple emulsions also show promise as delivery systems in cosmetic and pharmaceutical products, as they could enable sustained release of encapsulated compounds as well as the co-encapsulation of incompatible materials[4–7].

In most cases, the preparation of W/O/W emulsions requires a combination of hydrophilic and hydrophobic surfactants to stabilize the W/O as well as the O/W interface, and also a two-step

emulsification process[8] which introduces many destabilization pathways and lead to emulsions with short-term stability[9–12]. Many formulation approaches have been deployed to improve stability[8,13]: sophisticated combinations of emulsifiers have been selected, the proportions of the two types of emulsifiers have been optimized, co-surfactants have been added… However, the complexity of their multi-step formulation route, the lack of control of emulsions morphology and encapsulation rate, as well as the necessity of using important amounts of surfactants to obtain stable multiple emulsions, are still a limitation to large-scale applications[14].

Recently, progress has been made in the bulk formulation process of multiple emulsions as a couple of studies have shown that they can be prepared using a one-step phase inversion mixing process and a single emulsifier. This emulsifier can be a diblock copolymer[15–18] as well as some nanoparticles[19–21]. Hanson et al. were the first to obtain long-term stability W/O/W emulsions stabilized by a diblock polypeptide[15]. Sun et al. also demonstrated the possibility to prepare stable multiple emulsions stabilized by a synthetic diblock copolymer via catastrophic phase inversion[22]. Modified silica particles were used by Binks et al. to prepare stable W/O/W Pickering emulsions[19]. Li et al. were the first to use a single anionic surfactant to prepare stable W/O/W emulsions via catastrophic phase inversion[23]. Recently, Tu et al. also prepared one-step pH-responsive multiple emulsions via transitional phase inversion using Janus particles as a stabilizer[24].

A few years ago, our team proved that appropriate polymer architectures can easily generate one-step W/O/W emulsions via transitional phase inversion[17,25]. Water-toluene emulsions were stabilized using PS-*b*-P(S-*st*-DMAEMA) copolymers constituted of a hydrophobic block of polystyrene (PS) and a hydrophilic block of randomly distributed units of styrene (30 mol %) copolymerized with 2-(dimethylamino)ethyl methacrylate (DMAEMA) (70 mol %). Emulsions stabilized with these copolymers were stable for several months but were also

stimuli-responsive with a capacity of encapsulation tuned by pH or temperature[17,25]. The latter study showed that the architecture of the polymer is important for the stabilization of multiple emulsions. A study of polymer conformations based on Cryo-TEM imaging and SANS measurements also evidenced the link existing between interfacial curvature and emulsion type[25].

In this work, we describe another step forward by extending such advances to biocompatible systems. We used Atom Transfer Radical Polymerization to synthesize an amphiphilic PDMS-*b*-PDMAEMA diblock copolymer composed of a hydrophobic block of polydimethylsiloxane (PDMS) and a hydrophilic block of pure DMAEMA. PDMS and PDMAEMA polymers are materials which have already been demonstrated biocompatible properties and were used as micelles for anticancer drug delivery[26,27]. We used this pH, ionic strength and temperature-sensitive polymer to stabilize water - Miglyol® 812 as well as water – isopropyl myristate emulsions. Miglyol® 812 and isopropyl myristate are biocompatible oils widely used in pharmaceutics and cosmetics. With both systems, we show that stable W/O/W emulsions can be generated in a one-step formulation process via transitional phase inversion with pH and / or ionic strength. Finally, we investigate the formation of W/O/W emulsions through surface tension measurements and Cryo-TEM imaging to correlate multiple emulsion formation to tension and curvature of the interface.

EXPERIMENTAL SECTION

Materials. Monohydroxyl terminated poly(dimethylsiloxane) (number average molar mass 3000 $g.mol^{-1}$) (PDMS-OH), bromo-2-methylpropionyl bromide (BrMPBr, 98%), triethylamine (Et_3N, 99.5%), anhydrous tetrahydrofuran (THF, 99.9%), 1,1,4,7,10,10-hexamethyltriethylenetetramine (HMTETA, 97%), copper (I) bromide (CuBr, 99.999%), sodium hydrogenocarbonate ($NaHCO_3$, 99%), magnesium sulfate, sodium chloride (NaCl),

sodium nitrate ($NaNO_3$), isopropyl myristate and Nile Red were purchased from Sigma-Aldrich. 2-(dimethylamino)ethyl methacrylate (DMAEMA, 99%) and dichloromethane (99%) were obtained from Acros Organics. Miglyol® 812 was generously provided by IMCD. HCl and NaOH solutions were supplied by Merck. Milli-Q water with a resistivity of 18.2 MΩ.cm was used to prepare aqueous solutions for emulsions.

All reagents were used without further purification except the DMAEMA and the THF, which were filtered through a column of basic alumina (Acros Organics) to remove inhibitors and stabilizers and stored at low temperature, at – 10°C.

Synthesis of PDMS-*b*-PDMAEMA Block Copolymers. The block copolymer was synthesized by Atom Transfer Radical Polymerization (ATRP) of DMAEMA using preformed functional-PDMS. The scheme of the synthesis for PDMS-*b*-PDMAEMA is described in Figure 1. The PDMS-macroinitiator was synthesized from monohydroxyl-terminated-PDMS (PDMS-OH) according to a previously described procedure[28,29] with slight changes as reported below. Briefly, the PDMS macroinitiator was prepared from hydroxyl-terminated PDMS by using bromo-2-methylpropionyl bromide dissolved in anhydrous THF ($[PDMS\text{-}OH]_0$ = 0.16M) and triethylamine ($[Et3N]_0$ = 0.66M). Bromo-2-methylpropionyl bromide ($[BrMPBr]_0$ = 0.44M) was added and the reaction was stirred at room temperature for three days. Temperature was then increased and maintained at 60°C for one hour. The polymer solution was filtered to remove salts and the solvent was removed under vacuum. The resulting oil was dissolved in dichloromethane and washed with saturated $NaHCO_3$ aqueous solution and water. The organic phase was finally dried over magnesium sulfate, filtered and the solvent was removed under vacuum. Yield: 73%. ^1H NMR (400MHz,$CDCl_3$): 0 (s, 372H, Si-$(CH_3)_2$), 0.45 (t, 4H, Si-CH_2), 0.8 (t, 3H, CH_3), 1.2 (m, 4H, CH_2), 1.55 (m, 2H, CH_2), 1.9 (s, 6H, CH_3), 3.35 (t, 2H, CH_2-O), 3.65 (t, 2H, CH_2-O), 4.25 (t, 2H, CH_2-O-C=O).

Typically, Atom Transfer Radical Polymerizations (ATRP) were carried out under nitrogen atmosphere using syringe techniques. The catalyst (copper (I) bromide, 0.453 g, 0.32 mmol) was introduced in a dry round flask equipped with a three-way stopcock and a magnetic stirrer. Three nitrogen/vacuum cycles were performed. Monomer (DMAEMA, 2.44 g, 15.5 mmol), PDMS-macroinitiator (1.55 g, 0.52 mmol), soluble ligand (HMTETA, 0.158 g, 0.68 mmol) and solvent (THF, 50% of total volume) were bubbled with nitrogen and then added in a separated flask containing CuBr using a previously flame-dried stainless cannula. The polymerization of DMAEMA was then conducted under nitrogen at 60°C under magnetic stirring for three hours. Ratios between PDMS-macroinitiator, DMAEMA, CuBr and HMTETA were 1/30/1.3/2.6 respectively. The polymerization reaction was stopped by cooling down the flask under cold running water and the polymer solution was purified by passing through a column of basic alumina to remove copper. The excess of solvent was removed under vacuum and the polymer solution was precipitated in basic water to obtain a solid, which was then dried under vacuum.

Emulsions Preparation. The polymer was dissolved at the concentration of 5 $g.L^{-1}$ in either Miglyol® 812 or isopropyl myristate. NaCl, HCl and NaOH solutions were used to prepare aqueous solutions at different pH and ionic strengths using MilliQ-water. A fixed amount of 3 mL of polymer-containing oil and 3 mL of aqueous solution were placed into contact at room temperature for 24 hours before emulsification. All the pH values reported in this work were measured after 24 hours of contact between both phases. Emulsions were then obtained by mixing both phases using an Ultra Turrax T10 homogenizer (8 mm head) operating at 24000 rpm for 40 seconds.

Stability Measurements. Emulsion stability was assessed one day, one week, one month and two months after emulsification. Macroscopic stability was assessed by visual analysis of the vials containing emulsions. Emulsions are considered to be macroscopically stable as long as

the dispersed phases do not form a subnatant or supernatant phase separated from the emulsion. Microscopic stability was assessed by confocal microscopy. Emulsion pictures were taken at different times after emulsification and the mean diameter of emulsion drops was calculated for each picture. After emulsification, emulsion samples were stored in the dark at room temperature.

Characterization. Size Exclusion Chromatography (SEC, Viscotek GPC max VE2001; TDA 302 triple detector array) in THF containing 2% triethylamine and ^{1}H NMR spectroscopy (Bruker 400MHz spectrometer) were used to determine molar masses, polydispersity index (PDI) and precise compositions of block copolymer.

Residual copper in block copolymer samples was determined using i Cap Q-inductively coupled plasma-mass spectrophotometer from Thermo Elemental. Samples were prepared by solubilization of 20 mg of polymer in 30mL HNO_3 0.2M.

Confocal Laser Scanning Microscopy (CLSM) was used to determine emulsion type and stability. Confocal imaging was done in a quartz cell (0.5 mm light path) through an Olympus Fluoview FV1000 inverted confocal microscope. 150 µL emulsion samples were placed in the cell and studied at room temperature. Nile Red was used as a hydrophobic fluorophore, and the oil phase appear in blue in the pictures.

We used the following criterium to discriminate between O/W and W/O/W emulsions (O/W and W/O/W emulsions are identified by blue squares and green circles respectively in the emulsion type diagram). W/O/W emulsions are defined as emulsions for which the surface of the oil drops containing water droplets covers more than 50% of the surface of the emulsion, the surfaces being measured from a series of four confocal microscopy pictures of a given sample. If the criterium is not fulfiled, the emulsions are called O/W.

Diameters of emulsions drops were calculated from the images obtained by confocal microscopy. For each W/O/W emulsion, we measured the mean drop size and standard deviation (SD) of a panel of 500 oil globules using ImageJ (NIH software) with a systematic error of 10 %, mostly because some drops are visible albeit their largest diameter is not perfectly in the z plane of focus.

Interfacial tensions were measured using a spinning drop tensiometer (SVT 20N, Dataphysics). Measures were made on pre-equilibrated samples for 24 hours in presence of polymer, for different pH and ionic strengths. A capillary was filled with the equilibrated aqueous phase, avoiding formation of air bubbles and a small drop of the oil phase was formed into the capillary using a syringe. The elongation of the oil droplet stops when the centrifugal forces are balanced by the interfacial tension forces. By measuring the cylinder radius, the interfacial tension was determined from the Vonnegut's equation[30]. For each pH and ionic strength condition, the measure was repeated at least two times.

Morphology of structures formed by the copolymer in aqueous phases after partitioning was determined from Cryo-TEM images. Drops of aqueous phase were deposited on EM grids covered with a holly carbon film (Quantifoil R2/2) previously treated by plasma glow discharge. The excess of liquid on the grids was blotted out with a filter paper and the grids were quickly immerged in liquid ethane to form a thin vitreous ice film. The whole process was performed using a Vitrobot apparatus (PEI Company). Observations were conducted at low temperature (-180°C) on a JEOL 2010 FEG microscope operated at 200 kV. The contrast arises from the differences in the electron densities of the sample molecules. The defocus was set to 7 000 – 10 000 nm to obtain enough phase contrast under low-dose conditions. Images were recorded with a Gatan camera.

RESULTS AND DISCUSSION

Synthesis of PDMS-*b*-PDMAEMA Block Copolymer. The PDMS-*b*-PDMAEMA diblock copolymer was synthesized by ATRP from a preformed PDMS-macroinitiator. We used commercially available monohydroxyl terminated PDMS as a starting material to obtain a monofunctional bromoalkyl-terminated PDMS-macroinitiator suitable for the polymerization of DMAEMA by ATRP (Figure 1).

The PDMS-macroinitiator is obtained by simple condensation reaction of well-defined hydroxyl terminated PDMS with BrMPBr[28,29], which has been used in a subsequent step for the polymerization of DMAEMA by ATRP (Figure 1). The copper-mediated living radical polymerization of DMAEMA from PDMS-macroinitiator was carried out in THF (DMAEMA/THF, 1/1 vol.) at 60°C. The target molar mass of PDMAEMA block is 5 500 $g.mol^{-1}$ and [DMAEMA]/[PDMS-macroinitiator]/[CuBr]/[HMTETA] were 30/1/1.3/2.6.

The number average molar mass of PDMS-*b*-PDMAEMA and the polymer composition were determined by ^1H NMR (Figure 2). First, the number average molar mass of the PDMS-macroinitiator was estimated by ^1H NMR to be around 3000 $g.mol^{-1}$ corresponding to a polymerization degree of 38 (^1H NMR spectrum not shown). The methacrylate content in the PDMS-*b*-PDMAEMA copolymer was determined from the relative intensities of protons characteristic of the PDMAEMA (singlets assigned to both of CH_2 groups and the $N(CH_3)_2$ group from PDMAEMA at 2.6 and 4.1 as well as 2.3 ppm, respectively) and PDMS (singlet assigned to both of CH_3 groups at 0 ppm) blocks. As a result, the PDMS-*b*-PDMAEMA block copolymer was designed by $PDMS_{38}$-*b*-$PDMAEMA_{25}$.

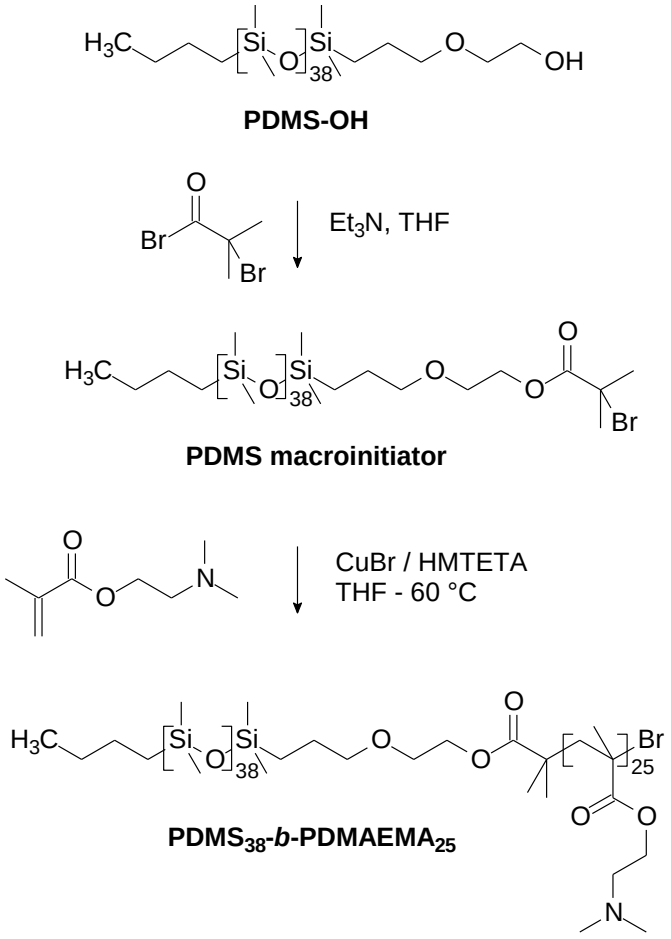

Figure 1. Synthesis of a PDMS-b-PDMAEMA block copolymer from a monohydroxyl-terminated PDMS.

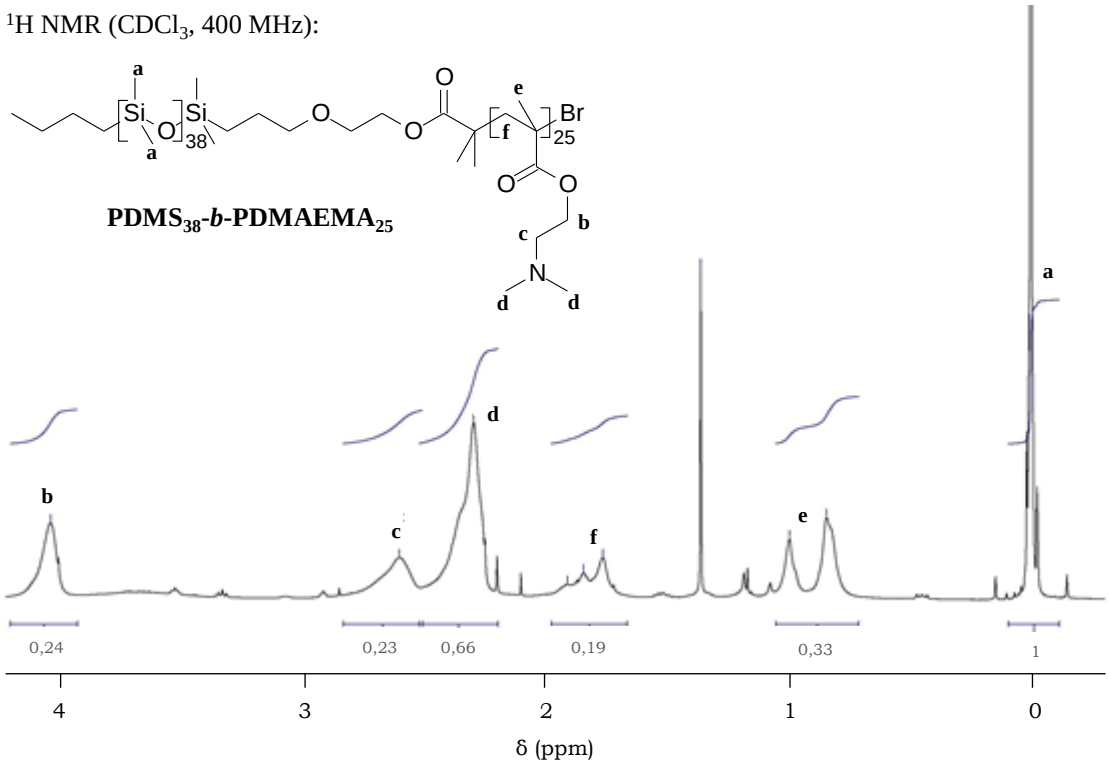

Figure 2. ^{1}H NMR spectra of $PDMS_{38}$-*b*-$PDMAEMA_{25}$ in $CDCl_3$

The narrow unimodal molar mass distribution of $PDMS_{38}$-*b*-$PDMAEMA_{25}$ was evidenced by SEC analysis with the PDI = 1.2 (Figure 3). The quantitative shift of $PDMS_{38}$-*b*-$PDMAEMA_{25}$ SEC trace to higher molar mass corresponding to a lower retention volume demonstrates the high efficiency of the initiation step from PDMS-macroinitiator. Copper synthesis residues were analyzed by ICP-MS and a concentration of 3.4×10^{-4} copper ion per chain was measured for the $PDMS_{38}$-b-$PDMAEMA_{25}$ copolymer.

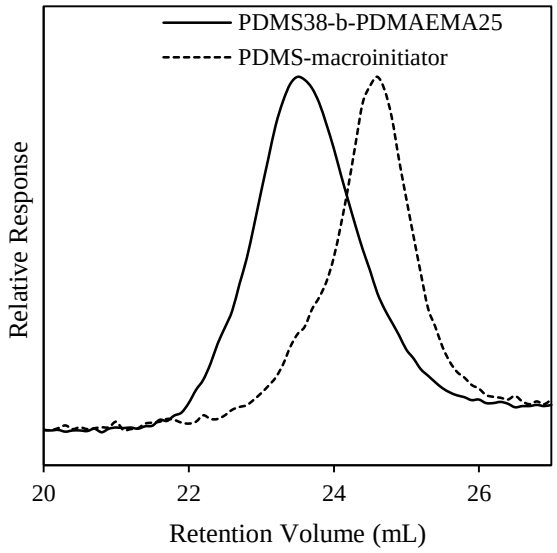

Figure 3. SEC traces of $PDMS_{38}$-*b*-$PDMAEMA_{25}$ and its PDMS-macroinitiator

Emulsions Formulated Without Polymer. Water – Miglyol® 812 and water – isopropyl myristate (1/1 vol.) emulsions were made without the addition of any emulsifier for different conditions of pH and ionic strength (*I*). Both oils have a slight surface-active effect and stable O/W emulsions were obtained in both cases. The pH and ionic strength domains where these emulsions form are represented on Figure 4. Emulsions made at pH = 10 are stable for several weeks whereas the water – Miglyol® 812 one formed at pH = 6 is stable for only a few minutes.

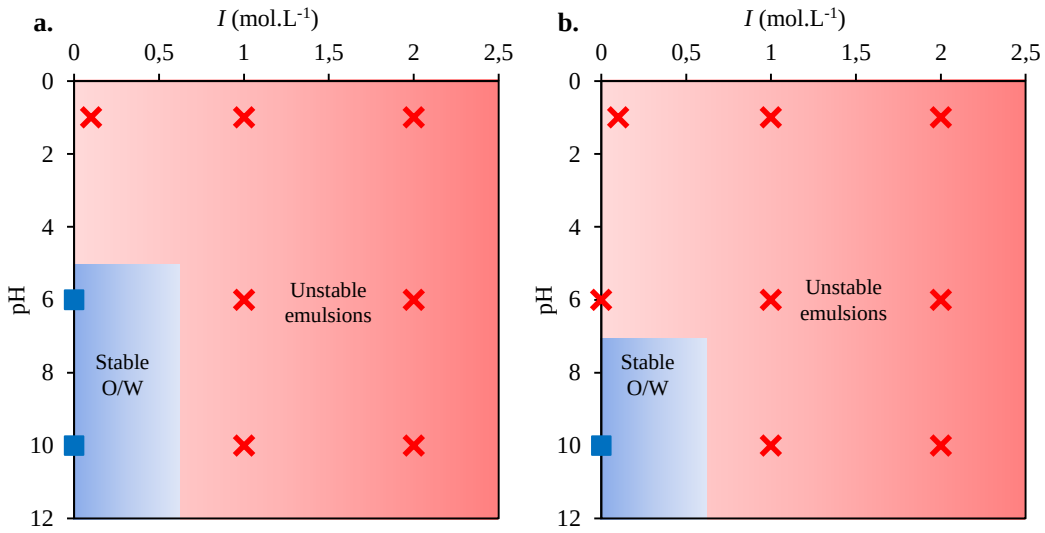

Figure 4. Stability domains of the O/W emulsions formulated with **a.** Miglyol® 812 and **b.** isopropyl myristate as emulsifiers.

One-Step Formation of Water – Miglyol® 812 Emulsions Stabilized by PDMS$_{38}$-*b*-PDMAEMA$_{25}$. Water – Miglyol® 812 (1/1 vol.) emulsions stabilized by PDMS$_{38}$-*b*-PDMAEMA$_{25}$ were generated in one emulsification step at constant mixing power. Emulsions were made at different conditions of pH and ionic strength, and emulsion type was determined by confocal microscopy. The effect of ionic strength and pH on emulsion morphology is summarized in emulsion type diagrams in Figures 5.a and 5.b right after and two months after preparation respectively. Table 1 presents mean drop diameters and standard deviations for W/O/W emulsions at both times.

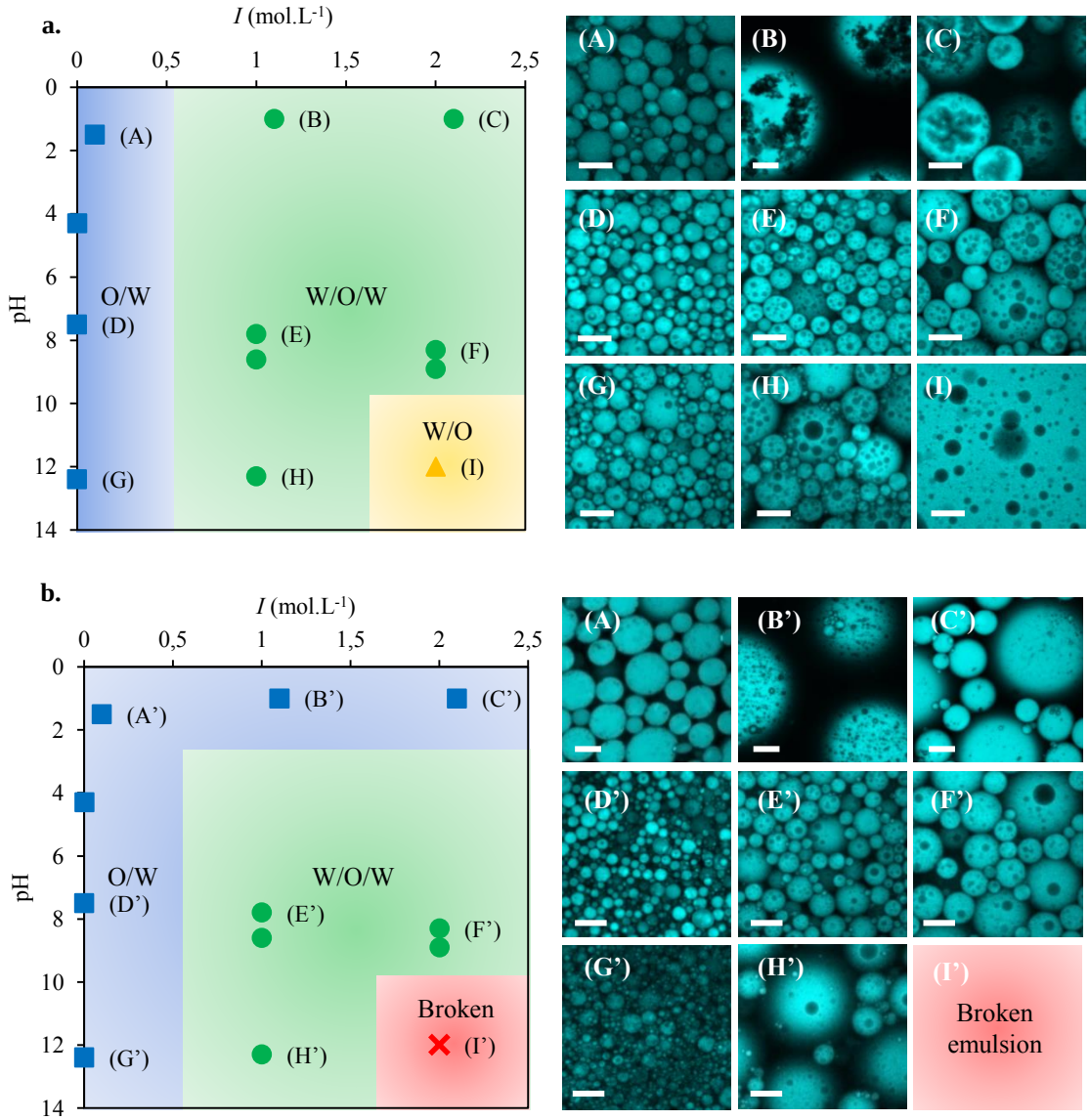

Figure 5. Emulsion type diagrams and fluorescence confocal microscopy images for water – Miglyol® 812 emulsions stabilized by $PDMS_{38}$-*b*-$PDMAEMA_{25}$ **a.** immediately after and **b.** two months after emulsification. Emulsion type diagrams present the following domains: O/W (squares), W/O/W (circles), W/O (triangles) and broken (crosses) emulsions. The oil phases appear in blue, all scales bars are 30 µm, except for emulsions **(B)**, **(A')**, **(B')** and **(C')** for which the scale bar is 100 µm.

Sample (t = 0)	B	C	E	F	H
Mean diameter / SD (µm)	206/65	58/18	19/6	30/14	38/20
Sample (t = 2 months)			E'	F'	H'
Mean diameter / SD (µm)	-	-	19/7	30/16	51/25

Table 1. Comparison of mean oil drop diameter and standard deviation (SD) just after and two months after emulsification for water - Miglyol® 812 W/O/W emulsions stabilized by $PDMS_{38}$-*b*-$PDMAEMA_{25}$. The error in the determination of mean oil drop diameters can be estimated to be around 10 %. Only oil globules were taken into account for the determination of mean drop diameter and SD.

Directly after emulsification, three different types of emulsions are obtained: O/W emulsions at low ionic strength, W/O emulsions at very high pH and ionic strength and W/O/W on the rest of the diagram.

When no salt is added to the aqueous phase, other than the salt necessarily introduced to control the pH, only O/W emulsions are formed on the whole pH range (Figure 5.a, **(A)**, **(D)** and **(G)**). The fact that no multiple emulsions are formed with this system is consistent with the architecture of the polymer used in this study since previous results on other systems[25] have shown that no multiple emulsions are formed when the hydrophilic block of the copolymer is purely constituted of DMAEMA. Here, it is also found out that no pH-driven phase inversion takes place for this system at $I = 0$ mol.L^{-1}. This is probably amplified by the surface-active effect of the oil which acts like a hydrophilic surfactant in this pH and I conditions and thus promotes the stabilization of O/W emulsions only.

At pH > 10 and I > 1.5 mol.L^{-1}, the formation of W/O emulsions is observed (Figure 5.a, **(I)**). At this basic pH, the polymer is fully neutralized and the high ionic strength contributes to increasing the hydrophobicity of the polymer[31]. The extension of the hydrophilic block of the copolymer is then significantly reduced, and could become smaller than the extension of the hydrophobic block. Such conditions are likely to promote an interface curvature towards water and thus the stabilization of W/O emulsions.

Finally, a remarkably large domain is evidenced in which stable W/O/W emulsions are formulated (Figure 5.a, **(B)**, **(C)**, **(E)**, **(F)** and **(H)**). These W/O/W emulsions are readily formed in one emulsification step using a single polymeric emulsifier at pH and ionic strength conditions intermediate to those that lead to the formation of O/W and W/O emulsions. A control over a wide range of oil droplet sizes is reached by adjusting the conditions of pH and ionic strength of the water phase at constant mixing power. Indeed the mean diameter for the oil drops of the W/O/W emulsions decreases from 200 µm for emulsion **(B)** to 19 µm for emulsion **(E)** (Table 1). Recently, Bae et al.[32] described a mechanism to explain the formation of W/O/W emulsions in a two-step emulsification process. The first one is the making of a simple O/W emulsion by mixing and the second one consists in the spontaneous formation of the W/O/W emulsion by inner water drops formation. In the second step, water transfers to the oil under the osmotic pressure gradient caused by the presence of salt residues in oil, which are however more soluble in water than in oil. Consequently, in Bae's mechanism, a growing kinetics of the inner water drops leading to the formation of monodisperse water drops with final size controlled by the amount of salt both in oil and water is observed. In our case, the inner water droplets of our W/O/W emulsions are immediately visible after preparation and no growth kinetics is observed. Moreover our water drops size polydispersity is rather large in sharp contrast with Bae's observations. Although quite interesting, we then believe that Bae's mechanism is not sufficient to explain the formation of our W/O/W. It is

thus reasonable to admit that there might be some other underlying mechanism(s) that takes place to explain the W/O/W emulsion formation in our systems. Also, the polymers used here (PDMS-b-PDMAEMA) was synthesized by ATRP and contain copper residues at a concentration of 3.4 x 10^{-4} copper ions per chain. The copper concentration is thus ten times lower than the concentration of Bae's purest copolymer where multiple emulsions do not form. Consequently, the formation of multiple emulsions is unlikely due to this mechanism only in our case.

Two months after emulsification all emulsions are still macroscopically stable, to the exception of the W/O one (Figure 5, **(I')**), which separates into oil and aqueous phases. The O/W domain has also enlarged at the expense of the W/O/W emulsion one. More precisely, the multiple emulsions prepared at pH = 1 were turned into O/W ones, irrespective of ionic strength (Figures 5.b, **(B')** and **(C')**). In particular, for all emulsions prepared at pH = 1, oil droplets have coarsened with a diameter increase of about 30% (Table 1), showing a lack of microscopic stability. However, all other W/O/W emulsions (Figure 5.b **(E')**, **(F')** and **(G')**) present excellent macroscopic and microscopic stability, especially emulsions **(E')** and **(F')**, which show comparable water encapsulation and similar sizes of the oil globules after emulsification and two months later (Table 1).

One-Step Formation of Water – Isopropyl Myristate Emulsions Stabilized by $PDMS_{38}$-*b*-$PDMAEMA_{25}$. Similar emulsion type diagrams were obtained with isopropyl myristate as the oil phase just after (Figure 6.a) and two months after emulsification (Figure 6.b). Table 2 presents mean drop diameters and standard deviations for W/O/W emulsions at both times.

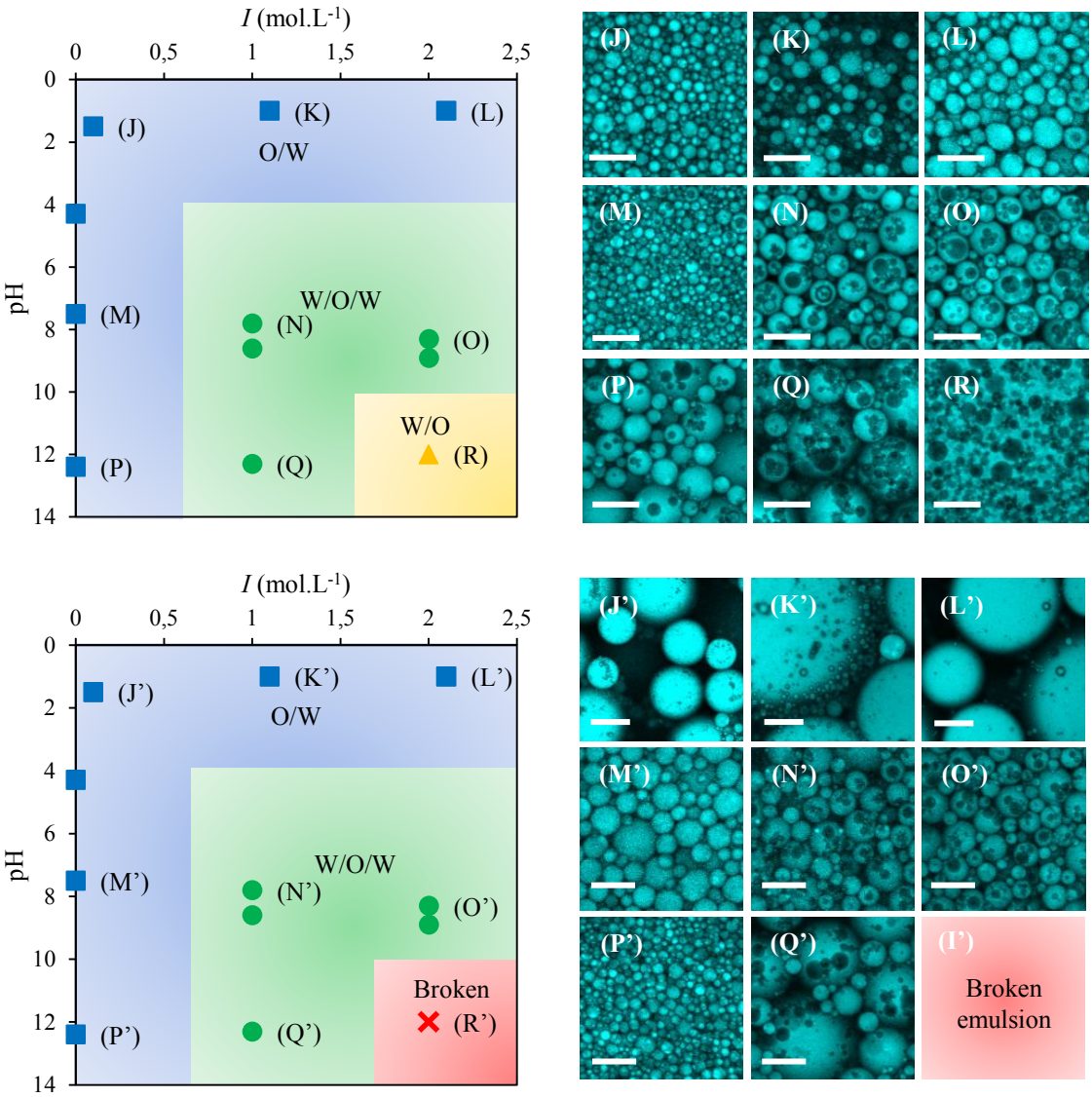

Figure 6. Emulsion type diagrams and fluorescence confocal microscopy images for water – isopropyl myristate emulsions stabilized by $PDMS_{38}$-*b*-$PDMAEMA_{25}$ **a.** immediately after and **b.** two months after emulsification. Emulsion type diagrams present the following domains: O/W (squares), W/O/W (circles), W/O (triangles) and broken (crosses) emulsions. The oil phases appear in blue, all scales bars are 30 µm, except for emulsions **(J')**, **(K')** and **(L')** for which the scale bar is 100 µm.

Sample (t = 0)	N	O	Q
Mean diameter / SD (µm)	14/6	15/6	23/13
Sample (t = 2 months)	N’	O’	Q’
Mean diameter / SD (µm)	13/5	14/5	25/12

Table 2. Comparison of mean oil drop diameter and standard deviation (SD) just after and two months after emulsification for water – isopropyl myristate W/O/W emulsions stabilized by $PDMS_{38}$-*b*-$PDMAEMA_{25}$. The error in the determination of mean oil drop diameters can be estimated to be around 10 %. Only oil globules were taken into account for the determination of mean drop diameter and SD.

For water – isopropyl myristate emulsions stabilized by $PDMS_{38}$-*b*-$PDMAEMA_{25}$, only O/W emulsions were obtained without addition of external salt on the whole pH range (Figure 6 **(J)**, **(M)** and **(P)**), as it was the case for the water - Miglyol® 812 ones (Figure 5, **(A)**, **(D)** and **(G)**). As we remarked previously, this is consistent with the architecture of the polymer and with the surface-active effect of the oil (Figure 4).

For this system, all emulsions formed at pH = 1 are O/W ones as soon as the emulsification has taken place (Figure 6, **(J)**, **(K)** and **(L)**). These emulsions present a limited microscopic stability (Table 2). At high pH and *I*, unstable W/O emulsions are formed (Figure 6, **(R)**).

At intermediate values of pH and *I*, a large domain of stable W/O/W emulsions is obtained (Figure 6, **(N)**, **(O)** and **(Q)**). These emulsions display excellent macroscopic and microscopic stability (Table 2), but it can be seen on the confocal microscopy pictures that the internal water droplets have flocculated inside oil globules, showing that the water – myristate – $PDMS_{38}$-*b*-$PDMAEMA_{25}$ system is less efficient than the water – Miglyol® 812 – $PDMS_{38}$-*b*-

$PDMAEMA_{25}$ at stabilizing the W/O interface of W/O/W emulsions. This can be due to the increased density difference between isopropyl myristate and water compared to Miglyol® 812, which causes the internal droplets to sediment inside the oil globules and promote flocculation.

Study of Interfacial Tensions between Oil and Water in Presence of Polymer. To get insight on emulsion type diagrams, interfacial tensions between both oils and water in the presence of $PDMS_{38}$-*b*-$PDMAEMA_{25}$ were measured for different values of pH and ionic strength (Table 3).

Miglyol® 812	(A)	(B)	(C)	(D)	(E)	(F)	(G)	(H)	(I)
γ ($mN.m^{-1}$)	2.0±0.4	2.0±0,4	4.7±1.0	1.1±0.2	1.5±0.3	0.9±0.2	2.1±0.4	1.4±0.3	0.8±0.2
Isopropyl myristate	(J)	(K)	(L)	(M)	(N)	(O)	(P)	(Q)	(R)
γ ($mN.m^{-1}$)	0.4±0.1	1.6±0.3	3.6±0.8	3.8±0.8	0.3±0.1	0.4±0.1	2.0±0.4	1.4±0.3	0.5±0.1

Table 3. Values of interfacial tension between Miglyol® 812 and water in presence of $PDMS_{38}$-*b*-$PDMAEMA_{25}$ for different conditions of pH and ionic strengths.

For both oils, the variation in the interfacial tension values from one sample to another (Table 3) appears to be too small to make the interfacial tension a decisive parameter to determine the emulsion type or even the final size of the emulsion drops. Interfacial tensions for W/O/W emulsions are slightly smaller for isopropyl myristate (Table 3, **(N)** and **(O)**) than for Miglyol® 812 (Table 3, **(E)** and **(F)**), which may explain the smallest drop size for W/O/W emulsions stabilized by isopropyl myristate (Table 1 and 2).

Probing interfacial curvature with Cryo-TEM measurements. As it was previously suggested that interfacial curvature likely imposes the type of emulsion for W/O and O/W types[25], a reasonable assumption would be that the curvature of the water – oil interface in presence of polymer is close to zero in the domain where W/O/W are formed. Indeed, this could lead to the stabilization of both types of interfaces.

The nature of microemulsions formed in the aqueous phase after partitioning was determined using Cryo-TEM measurement (Figure 7). Cryo-TEM imaging was only carried out on water – isopropyl myristate microemulsions because no images could be obtained for water – Miglyol® 812 ones, which is probably related to an incompatibility between the nature of the oil and the freezing process.

Two cases were compared: one corresponding to O/W emulsion **(J)** (pH = 1, I = 0.1 mol.L^{-1}) and the other corresponding to W/O/W emulsion **(N)** (pH = 8, I = 1 mol.L^{-1}). In both cases, the $PDMS_{38}$-*b*-$PDMAEMA_{25}$ copolymer chains transfer enough in water to form aggregates detectable by Cryo-TEM. The presence of oil inside polymer micelles was previously confirmed by Small Angle Neutron Scattering for both systems (data not shown). For the sample corresponding to O/W emulsion **(J)**, aggregates are spherical, meaning that the $PDMS_{38}$-*b*-$PDMAEMA_{25}$ film curves towards oil, which is in agreement with the O/W type of emulsion obtained with this sample (Figure 7.a). On the contrary, for the sample corresponding to W/O/W emulsion **(N)**, detectable aggregates are a mixture of spherical and cylindrical micelles (Figure 7.b). The microemulsion morphology changes between the two samples can be attributed to modifications in the interfacial polymer layer. Indeed, microemulsions are usually well described as an assembly of flexible films dominated by the curvature energy as introduced by Helfrich[33]. It was indeed shown that for a certain range of the curvature parameters, a transition occurs from spherical to cylindrical micelles through a

region where both are present[34,35]. This transition is linked to a decrease of film curvature, in accordance with the change of emulsion type between the two samples. However, it appears that a non-zero positive curvature is compatible with the formation of multiple emulsions.

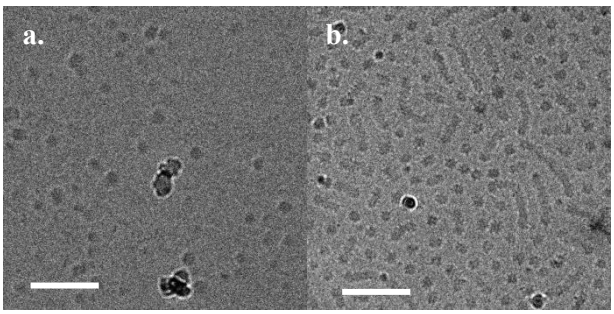

Figure 7. Cryo-TEM pictures of water – isopropyl myristate microemulsions formed in water in the presence of $PDMS_{38}$-*b*-$PDMAEMA_{25}$ **a.** Sample **(J)** and **b.** sample **(N)**. All scale bars represent 100 nm.

CONCLUSION

In this paper, we synthesized a biocompatible copolymer that can be used as a single emulsifier to stabilize W/O/W emulsions using two different biocompatible oils, isopropyl myristate and Miglyol® 812. These emulsions are formulated in a one-step emulsification process induced by transitional phase inversion using pH and ionic strength fine adjustments. The formulation of our system is indeed well-controlled and highly reproducible. It leads to the making of W/O/W emulsions with long-term stability in a large domain of pH and ionic strength conditions. The interfacial tension is not a key parameter to predict emulsion type even if the formation of multiple emulsions often requires low interfacial tensions. However, the tuning of the polymer films interfacial curvature and hence microemulsions morphology is likely to be a determinant parameter to promote emulsion type in general and in particular the formation of W/O/W emulsions.

AUTHOR INFORMATION

Corresponding Author. * E-mail: patrick.perrin@espci.fr ; patrick.guenoun@cea.fr

ACKOWLEDGEMENT

We thank the RTRA Triangle de la Physique for its funding through the Imagemul project. Cryo-TEM observations were done thanks to "Investissements d'Avenir" LabEx PALM (ANR-10-LABX-0039-PALM). We gratefully acknowledge Mohamed Hanafi for the SEC analysis. We thank IMCD for having generously provided the Miglyol® 812 we used in our experiments.

REFERENCES

(1) Muschiolik, G. Multiple Emulsions for Food Use. *Curr. Opin. Colloid Interface Sci.* **2007**, *12* (4–5), 213–220.
(2) O'Regan, J.; Mulvihill, D. M. Sodium Caseinate–Maltodextrin Conjugate Stabilized Double Emulsions: Encapsulation and Stability. *Food Res. Int.* **2010**, *43* (1), 224–231.
(3) Jiménez-Colmenero, F. Potential Applications of Multiple Emulsions in the Development of Healthy and Functional Foods. *Food Res. Int.* **2013**, *52* (1), 64–74.
(4) Gallarate, M.; Carlotti, M. E.; Trotta, M.; Bovo, S. On the Stability of Ascorbic Acid in Emulsified Systems for Topical and Cosmetic Use. *Int. J. Pharm.* **1999**, *188* (2), 233–241.
(5) Carlotti, M. E.; Gallarate, M.; Sapino, S.; Ugazio, E.; Morel, S. W/O/W Multiple Emulsions for Dermatological and Cosmetic Use, Obtained with Ethylene Oxide Free Emulsifiers. *J. Dispers. Sci. Technol.* **2005**, *26* (2), 183–192.
(6) Schwarz, J. C.; Klang, V.; Karall, S.; Mahrhauser, D.; Resch, G. P.; Valenta, C. Optimisation of Multiple W/O/W Nanoemulsions for Dermal Delivery of Aciclovir. *Int. J. Pharm.* **2012**, *435* (1), 69–75.
(7) Hoppel, M.; Mahrhauser, D.; Stallinger, C.; Wagner, F.; Wirth, M.; Valenta, C. Natural Polymer-Stabilized Multiple Water-in-Oil-in-Water Emulsions: A Novel Dermal Drug Delivery System for 5-Fluorouracil: W/O/W for 5-Fluorouracil. *J. Pharm. Pharmacol.* **2014**, *66* (5), 658–667.
(8) Garti, N. Double Emulsions - Scope, Limitations and New Achievements. *Colloids Surf. Physicochem. Eng. Asp.* **1997**, *123–124*, 233–246.
(9) Dobrynin, A. V.; Colby, R. H.; Rubinstein, M. Scaling Theory of Polyelectrolyte Solutions. *Macromolecules* **1995**, *28* (6), 1859–1871.
(10) Ficheux, M.-F.; Bonakdar, L.; Leal-Calderon, F.; Bibette, J. Some Stability Criteria for Double Emulsions. *Langmuir* **1998**, *14* (10), 2702–2706.
(11) Garti, N.; Benichou, A. Recent Developments in Double Emulsions for Food Applications. *Food Emuls.* **2004**, *35*.

(12) Jiao, J.; Burgess, D. J. Multiple Emulsion Stability: Pressure Balance and Interfacial Film Strength. In *Multiple Emulsions*; Aserin, A., Ed.; John Wiley & Sons, Inc., 2007; pp 1–27.
(13) Garti, N.; Bisperink, C. Double Emulsions: Progress and Applications. *Curr. Opin. Colloid Interface Sci.* **1998**, *3* (6), 657–667.
(14) Dickinson, E. Double Emulsions Stabilized by Food Biopolymers. *Food Biophys.* **2011**, *6* (1), 1–11.
(15) Hanson, J. A.; Chang, C. B.; Graves, S. M.; Li, Z.; Mason, T. G.; Deming, T. J. Nanoscale Double Emulsions Stabilized by Single-Component Block Copolypeptides. *Nature* **2008**, *455* (7209), 85–88.
(16) Hong, L.; Sun, G.; Cai, J.; Ngai, T. One-Step Formation of W/O/W Multiple Emulsions Stabilized by Single Amphiphilic Block Copolymers. *Langmuir* **2012**, *28* (5), 2332–2336.
(17) Besnard, L.; Marchal, F.; Paredes, J. F.; Daillant, J.; Pantoustier, N.; Perrin, P.; Guenoun, P. Multiple Emulsions Controlled by Stimuli-Responsive Polymers. *Adv. Mater.* **2013**, *25* (20), 2844–2848.
(18) Zhang, Y.; Gou, J.; Sun, F.; Geng, S.; Hu, X.; Zhang, K.; Lin, X.; Xiao, W.; Tang, X. Impact of Electrolytes on Double Emulsion Systems (W/O/W) Stabilized by an Amphiphilic Block Copolymer. *Colloids Surf. B Biointerfaces* **2014**, *122*, 368–374.
(19) Binks, B. P.; Rodrigues, J. A. Types of Phase Inversion of Silica Particle Stabilized Emulsions Containing Triglyceride Oil. *Langmuir* **2003**, *19* (12), 4905–4912.
(20) Binks, B. P.; Whitby, C. P. Silica Particle-Stabilized Emulsions of Silicone Oil and Water: Aspects of Emulsification. *Langmuir* **2004**, *20* (4), 1130–1137.
(21) Binks, B. P.; Fletcher, P. D. I.; Thompson, M. A.; Elliott, R. P. Influence of Propylene Glycol on Aqueous Silica Dispersions and Particle-Stabilized Emulsions. *Langmuir* **2013**, *29* (19), 5723–5733.
(22) Sun, G.; Liu, M.; Zhou, X.; Hong, L.; Ngai, T. Influence of Asymmetric Ratio of Amphiphilic Diblock Copolymers on One-Step Formation and Stability of Multiple Emulsions. *Colloids Surf. Physicochem. Eng. Asp.* **2014**, *454*, 16–22.
(23) Li, Z.; Liu, H.; Zeng, L.; Liu, H.; Yang, S.; Wang, Y. Preparation of High Internal Water-Phase Double Emulsions Stabilized by a Single Anionic Surfactant for Fabricating Interconnecting Porous Polymer Microspheres. *Langmuir* **2014**, *30* (41), 12154–12163.
(24) Tu, F.; Lee, D. One-Step Encapsulation and Triggered Release Based on Janus Particle-Stabilized Multiple Emulsions. *Chem Commun* **2014**, *50* (98), 15549–15552.
(25) Besnard, L.; Protat, M.; Malloggi, F.; Daillant, J.; Cousin, F.; Pantoustier, N.; Guenoun, P.; Perrin, P. Breaking of the Bancroft Rule for Multiple Emulsions Stabilized by a Single Stimulable Polymer. *Soft Matter* **2014**, *10* (36), 7073–7087.
(26) Car, A.; Baumann, P.; Duskey, J. T.; Chami, M.; Bruns, N.; Meier, W. pH-Responsive PDMS-B-PDMAEMA Micelles for Intracellular Anticancer Drug Delivery. *Biomacromolecules* **2014**, *15* (9), 3235–3245.
(27) Dinu, I. A.; Duskey, J. T.; Car, A.; Palivan, C. G.; Meier, W. Engineered Non-Toxic Cationic Nanocarriers with Photo-Triggered Slow-Release Properties. *Polym Chem* **2016**, *7* (20), 3451–3464.
(28) Duquesne, E.; Habimana, J.; Degée, P.; Dubois, P. Synthesis of Silicone-Methacrylate Copolymers by ATRP Using a Nickel-Based Supported Catalyst. *Macromol. Chem. Phys.* **2006**, *207* (13), 1116–1125.
(29) Semsarzadeh, M. A.; Abdollahi, M. Atom Transfer Radical Polymerization of Styrene and Methyl (Meth)acrylates Initiated with Poly(dimethylsiloxane) Macroinitiator:

Synthesis and Characterization of Triblock Copolymers. *J. Appl. Polym. Sci.* **2012**, *123* (4), 2423–2430.
(30) Vonnegut, B. Rotating Bubble Method for the Determination of Surface and Interfacial Tensions. *Rev. Sci. Instrum.* **1942**, *13* (1), 6–9.
(31) Marchal, F.; Roudot, A.; Pantoustier, N.; Perrin, P.; Daillant, J.; Guenoun, P. Emulsion Stabilization and Inversion Using a pH- and Temperature-Sensitive Amphiphilic Copolymer. *J. Phys. Chem. B* **2007**, *111* (46), 13151–13155.
(32) Bae, J.; Russell, T. P.; Hayward, R. C. Osmotically Driven Formation of Double Emulsions Stabilized by Amphiphilic Block Copolymers. *Angew. Chem. Int. Ed.* **2014**, *53* (31), 8240–8245.
(33) Helfrich, W. Elastic Properties of Lipid Bilayers: Theory and Possible Experiments. *Z. Für Naturforschung Teil C Biochem. Biophys. Biol. Virol.* **1973**, *28* (11), 693–703.
(34) Pays, K.; Giermanska-Kahn, J.; Pouligny, B.; Bibette, J.; Leal-Calderon, F. Double Emulsions: A Tool for Probing Thin-Film Metastability. *Phys. Rev. Lett.* **2001**, *87* (17).
(35) Pays, K.; Mabille, C.; Schmitt, V.; Leal-Calderon, F.; Bibette, J. Understanding the Stability and Lifetime of Emulsions. *J. Dispers. Sci. Technol.* **2002**, *23* (1–3), 175–186.

TABLE OF CONTENT GRAPHIC